

# Thermostatistics of small non-linear systems: Poissonian athermal bath

Welles A. M. Morgado

*Department of Physics, PUC-Rio and  
National Institute of Science and Technology for Complex Systems  
Rua Marquês de São Vicente 225,  
22453-900 Rio de Janeiro — RJ, Brazil*

Sílvio M. Duarte Queirós

*Centro Brasileiro de Pesquisas Físicas and  
National Institute of Science and Technology for Complex Systems  
Rua Dr Xavier Sigaud, 150, 22290-180 Rio de Janeiro — RJ, Brazil*

## Abstract

We extend the study presented in [Phys. Rev. E **90**, 022110 (2014)] to the case of a small system subject to non-linear interaction and in contact with an athermal shot-noise reservoir. We first focus on steady state properties, namely on the impact of the singular measure of the reservoir in the steady state energy. Then, we introduce the concept of temperatures of higher-order, which aim to represent the effect produced by the cumulants of the noise of order larger than 2, and new response functions such as high-order specific heats, that zero out when the system is thermal or linear. Afterwards, we study the effect of the nature of the noise in the heat and energy fluxes and determine asymptotic expressions for its large deviation functions. Finally, in analysing the probabilistics of the injected power,  $j_{\text{inj}}$ , we verify that the exponential form of its fluctuation relation is only asymptotically valid whereas in the thermal case is valid for all  $j_{\text{inj}}$ .

**PACS:**02.50.Ey, 05.10.Gg, 05.60.-k

**Key-words:**Heat fluxes; coupled systems; white noise; shot-noise

## I. INTRODUCTION

The reasons for the assumption of a Wiener process to describe the stochastic term in the dynamical equations in statistical mechanics are well-known [1]. For instance, if one considers the quintessential non-equilibrium problem of the Brownian motion as studied by Einstein and Smoluchowski, we understand that the medium which acts as the thermal bath (or heat reservoir) is dense enough so that when an infinitesimal interval of time is assumed, the focal particle is in contact with a sufficiently large number of bath particles so that the statistics of the resultant of those collisions matches the central limit theorem. Therefore, the outcome of those interactions is split into the superposition of dissipative and stochastic contributions. The latter is responsible for the fluctuations and — according to what we have said — follows a Gaussian. Since both dissipation and fluctuations have the same origin and hence the fluctuation-dissipation relation is verified [2] that case is defined as a non-equilibrium internal reservoir system.

Nevertheless, when one has a closer look at the theory of stochastic processes, we realise the Wiener approach — which has a continuous measure — does only account for the continuous evolution of the state of a system that in probability space is described by the Fokker-Planck equation [3, 4]. That description utterly ignores possible jump contributions (eminently singular) to the master equation.

Complementarily, the Lévy-Itô theorem states that any white-noise process can be written as a superposition of a Wiener (continuous measure) and singular measure processes [5]. The latter is described by a Poisson process that corresponds to the addition of a sequence of pulses that take place at a rate,  $\lambda$ , which can be time dependent or not. Besides its relevance in the field of probability theory, the Poissonian shot-noise process is significant for the description of a series of physical cases: (i) solid state problems wherein shot (singular measure) noise is related to the quantization of the charge [6]; (ii) resistor-inductor-capacitor circuits with injection of power at some rate resembling heat pumps [7]; (iii) surface diffusion and low vibrational motion with adsorbates, e.g., Na/Cu(001) compounds [8]; (iv) biological motors in which shot noise mimics the non-equilibrium stochastic hydrolysis of adenosine triphosphate [9, 10]; (v) molecular dynamics when the Andersen thermostat is applied [11]; and (vi) little dense granular gases employed in ratchet systems [12–14].

Owing to problems related to heat transfer and thermostatics of small systems, the interest in shot-noise systems has recently stirred up. Particularly, in Ref. [15] and ulteriorly in Ref. [13], it was proved that its singular measure can have a major impact on the validity of thermodynamical principles as one usually state them, namely the law of heat conductance, if one neglects that shot-noise does not behave in a thermal way and consequently displays built-in important differences.

In this paper, we extend to white Poissonian shot-noise, which can be regarded as an athermal reservoir, the results we have obtained in Ref. [16] — hereinafter referred to as Paper I — for the thermostatics of a damped non-linear particle in contact with a thermal bath. The remaining of the paper is organised as follows: in Sec. 2 we introduce the relevant noise properties, the dynamical model we are going to study, the method of solution and previous results of ours for the linear case on the position and velocity that will be quite helpful in obtaining the results of the present manuscript; in Sec. 3 we present an steady state energetic analysis of the non-linear problem that includes a diagrammatic method for computing the cumulants of the position and we introduce new response functions; in Sec. 4, we first perform a time dependent study of the energy fluxes, namely the injected and dissipated fluxes, determining upper ( $\lambda \rightarrow \infty$ ) and lower bounds ( $\lambda \ll 1$ ) of the distributions which have the rôle of large deviation functions; afterwards, we analyse the distribution of the instantaneous injected power with the goal of understanding to what degree its thermal fluctuation relation is affected by the athermal nature of shot-noise; last, in Sec. 5, we present some final remarks over the results and provide some hints about future work.

## II. PRELIMINARIES

### A. Noise definition

The Poisson noise is defined by,

$$\eta(t) = \sum_{\ell} \Phi(t) \delta(t - t_{\ell}), \quad (1)$$

representing a set of events occurring at times,  $\{t_{\ell}\}$ , with a rate,  $\lambda(t)$ , and intensity,  $\Phi$ , related to a time independent distribution,  $f(\Phi)$ . Herein, we introduce results for typical

distributions, namely the exponential,

$$f(\Phi) = \Phi^{-1} \exp[-\Phi/\Phi], \quad (2)$$

( $\Phi > 0$ ) and the Gaussian,

$$f(\Phi) = (2\pi\sigma^2)^{-1/2} \exp[-\Phi^2/(2\sigma^2)]. \quad (3)$$

Please be aware that, in considering  $\Phi$  as Gaussian we are not defining a standard (thermal) reservoir, because we are keeping the shot-noise rate  $\lambda$  undefined and likely finite. Only in the limit  $\lambda$  going to infinity, we have  $\eta$  representing an instantaneous element of a Wiener process. For the sake of convenience, we focus on homogeneous Poisson processes,  $\lambda(t) = \lambda$ . A partial analysis of the statistics of the linear heterogeneous Poisson particle leading to stochastic resonance phenomena can be found in Ref. [17].

Assuming an independent generation of events, we have a white-noise process with its *cumulants* given by [18],

$$\langle\langle \eta(t_1) \dots \eta(t_n) \rangle\rangle \equiv \langle \Phi^n \rangle \lambda \prod_{i=1}^{n-1} \delta(t_{i+1} - t_i). \quad (4)$$

In our notation,  $\langle \mathcal{O}^n \rangle$  represents the raw  $n$ -th order statistical moment (averaged over samples) of  $\mathcal{O}$  and  $\langle\langle \mathcal{O}^n \rangle\rangle$  the respective cumulant. For the exponential and Gaussian typical cases we have  $\langle \Phi^n \rangle_{\text{exp}} = n! \Phi^n$  and  $\langle \Phi^{2n} \rangle_{\text{gauss}} = \sigma^{2n} (2n-1)!!$  (and zero otherwise), respectively.

Differently to the thermal reservoir, the shot-noise case demands considering all the cumulants be defined. As we will shortly find out, it is important to describe the noise cumulants in the reciprocal Laplace-Fourier space,

$$\mathcal{O}(iq + \epsilon) \equiv \int_0^\infty \mathcal{O}(t) e^{-(iq+\epsilon)t} dt, \quad (5)$$

which reads,

$$\begin{aligned} \langle\langle \eta(iq_1 + \epsilon) \dots \eta(iq_n + \epsilon) \rangle\rangle &= \int_0^\infty \prod_{i=1}^n dt_i \exp \left[ - \sum_{j=1}^n (iq_j + \epsilon) t_j \right] \langle\langle \eta(t_1) \dots \eta(t_n) \rangle\rangle \\ &= \lambda \langle \Phi^n \rangle \int_0^\infty dt_1 \exp \left[ - t_1 \sum_{j=1}^n (iq_j + \epsilon) \right] \\ &= \frac{\lambda \langle \Phi^n \rangle}{\sum_{j=1}^n (iq_j + \epsilon)}. \end{aligned} \quad (6)$$

## B. Dynamical model and linear results

Our system consists of a particle of mass  $m$  the dynamics of which is governed by the second-order differential equation,

$$m \ddot{x}(t) = -\gamma \dot{x}(t) - k_1 x(t) - k_3 [x(t)]^3 + \eta_t, \quad (7)$$

and velocity  $v \equiv \dot{x}$ , corresponding to a damped motion, which is more general than the usual overdamped approaches. In Eq. (7),  $\gamma$  represents the dissipation constant,  $k_1$  and  $k_3$  are the linear and non-linear coupling constants, respectively, and  $\eta$  denotes the stochastic interaction between the particle and the reservoir. Please heed that from Eqs. (4) and (7), we understand the dissipation and fluctuation spectra are the same and therefore this system is likely to verify a fluctuation-dissipation relation [2], as we will see soon. Nevertheless, we must pay attention to the fact that the Poissonian reservoir is not thermal and hence the standard internal reservoir classification is not entirely valid.

In probability space, Eq. (7) has as counterpart a jump Kramers-like integro-differential equation [3] describing the evolution of the joint probability density function  $f(x, v, t)$ .

The solution to that integro-differential equation is not accessible even in the generic linear case.<sup>1</sup> Therefore, in order to carry out a thermostistical analysis as inclusive as possible we must assume a different approach.

The dynamics allows the emergence of a steady state, *i.e.*, after a transient time of the order of  $m/\gamma$ , the statistics over time,  $\overline{\mathcal{O}^n}$ , matches that over samples,  $\langle \mathcal{O}^n \rangle$ , as well as the cumulants,  $\overline{\overline{\mathcal{O}^n}}$  and  $\langle\langle \mathcal{O}^n \rangle\rangle$ , computed therefrom. Hence, we can avail ourselves of the time averaging procedure based on the Fourier-Laplace transform and the final value theorem [21]. Under this approach, for  $x(0) = 0$  and  $v(0) = 0$ , Eq. (7) becomes (please check details in Sec. 2 of Paper I),

$$\tilde{x}(iq + \epsilon) = \frac{\tilde{\eta}(iq + \epsilon)}{R(iq + \epsilon)} - \frac{k_3}{R(iq + \epsilon)} \lim_{\epsilon \rightarrow 0^+} \int \int \int_{-\infty}^{\infty} \frac{dq_1}{2\pi} \frac{dq_2}{2\pi} \frac{dq_3}{2\pi} \frac{\tilde{x}(iq_1) \tilde{x}(iq_2) \tilde{x}(iq_3)}{q - (iq_1 + iq_2 + iq_3)}, \quad (8)$$

where,

$$R(w) \equiv m w^2 + \gamma w + k_1 = m (w - \zeta_+) (w - \zeta_-), \quad (9)$$

---

<sup>1</sup> A solution in the overdamped regime can be set up from the solution of a dragged linear shot-noise case presented in Ref. [10].

with,

$$\zeta_{\pm} = -\frac{\theta}{2} \pm \frac{i}{2}\Omega, \quad (10)$$

where  $\Omega \equiv \sqrt{4\omega^2 - \theta^2}$  and,

$$\theta = \frac{\gamma}{m}, \quad \omega^2 = \frac{k_1}{m}. \quad (11)$$

Note that all the (linear) mechanical information on the system is stored in the roots  $\zeta_{\pm}$  of  $R(w)$ . As introduced in Paper I, Eq. (8) can be represented in the form of the diagram in Fig. 1. In it, the recurrence relation given by Eq. (8) is drawn, where double line circles are a pictorial representation of  $\tilde{x}$  while the single line circle is a representation of  $\tilde{\eta}$ . The full black circle represents the integration and is used as a mnemonic device.

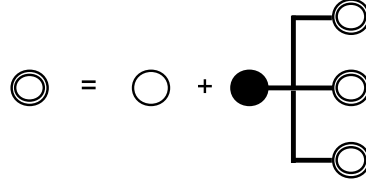


FIG. 1. Diagrammatic representation of Eq. (8) as introduced in Paper I.

The velocity in the reciprocal space is simply given by,

$$\tilde{v}(iq_1 + \epsilon) = (iq_1 + \epsilon) \tilde{x}(iq_1 + \epsilon). \quad (12)$$

Equation (11) shows that besides the time scale of relaxation,  $\tau_r \equiv \theta^{-1}$ , our problem has got two additional time scales: the scale of damped oscillation,  $\tau_o \equiv 2\pi\Omega^{-1}$ , and the scale of the shot-noise,  $\tau_n \equiv \lambda^{-1}$ . It is the trait  $\tau_n \neq 0^+$  that introduces a singular (athermal) character to the reservoir.

In solving the non-linear problem, we will consider it as a perturbation to the steady state linear case and thus it is worth making the statistics of  $x$  and  $v$  explicit as in Ref. [17]. Therein, we found that the cumulants of the position, obtained by time averaging for  $k_3 = 0$ , are given by the formula,

$$\overline{\overline{x^n}} = n! \frac{(-1)^{n+1}}{\prod_{j=0}^{n-1} [(n-j), j]} \frac{\lambda \langle \Phi^n \rangle}{m^n}. \quad (13)$$

where,

$$[a, b] \equiv a \zeta_+ + b \zeta_- . \quad (14)$$

Regarding the cumulants of the velocity, in the harmonic case we got,

$$\overline{v^n} = \sum_{j=0}^{n-1} (-1)^{j-1} \binom{n-1}{n-j-1} \frac{\zeta_+^{n-j-1} \zeta_-^j [(n-j-1), j]}{\prod_{l=0}^1 [(n-j-l), (j+l)]} \frac{\lambda \langle \Phi^n \rangle}{m^n [1, -1]^{n-1}} . \quad (15)$$

The computation of the position-velocity cross correlation function yields,

$$C_{xv}(s) = \exp \left[ -\frac{\gamma}{2m} |s| \right] \frac{\lambda \langle \Phi^2 \rangle}{m \gamma \Omega} \sin \left[ -\frac{1}{2} \Omega |s| \right] . \quad (16)$$

It is not difficult to verify that in the long term  $\bar{v} = 0$  as proper of a steady state.

It is clear that when measured at the same instant ( $s = 0$ ), the position and velocity are uncorrelated and thus the joint probability density function  $p(x, v) = p(x) p(v)$ .

Because for all  $n \geq 2$ , the cumulants  $\overline{x^n}$  and  $\overline{v^n}$  are generally different from zero, distributions  $p(x)$  and  $p(v)$  are not Gaussians. However, as we will learn, both marginal distributions converge to the Gaussian when the rate of events  $\lambda$  tends to infinity as jumps become a continuum of random kicks and the noise approaches a continuous measure.

### III. RESULTS FOR THE ENERGY

With the linear results in hand, we move on to the thermostistical analysis of the non-linear system by bridging the (average) kinetic energy,  $\mathcal{K}$ , and the (average) potential energy,  $\mathcal{V}$ , with the properties of the reservoir. The total (average) energy of the system,  $\mathcal{K} + \mathcal{V}$ , is denoted by  $\mathcal{E}$ . For some processes, even at low temperatures the classical energy will not converge to zero due to the linear cumulant of the Poisson noise. For these cases, we might offset the energy by the corresponding minimum  $\mathcal{E}_0 = \frac{\lambda^2 \langle \Phi \rangle^2}{2k_1^2}$ .

#### A. Kinetic energy and canonical temperature in the non-linear system

To obtain the kinetic energy, we must compute the average square velocity,

$$\overline{v^2} = \lim_{z, \epsilon \rightarrow 0} \int_{-\infty}^{\infty} \frac{dq_1}{2\pi} \int_{-\infty}^{\infty} \frac{dq_2}{2\pi} \frac{z}{z - (i q_1 + i q_2 + 2\epsilon)} (i q_1 + \epsilon)(i q_2 + \epsilon) \times [\langle \tilde{x}(i q_1 + \epsilon) \tilde{x}(i q_2 + \epsilon) \rangle] , \quad (17)$$

Plugging Eq. (8) into the last equation we separate out the linear,  $\overline{v^2_1}$ , and non-linear,  $\overline{v^2_{nl}}$ , terms and perform the calculations up to first order of  $k_3$ .<sup>2</sup> For the former we have,

$$\overline{v^2_1} = \frac{\lambda \langle \Phi^2 \rangle}{2m\gamma}, \quad (18)$$

whereas for the latter we verify that (see Appendix C)

$$\overline{v^2_{nl}} = 0. \quad (19)$$

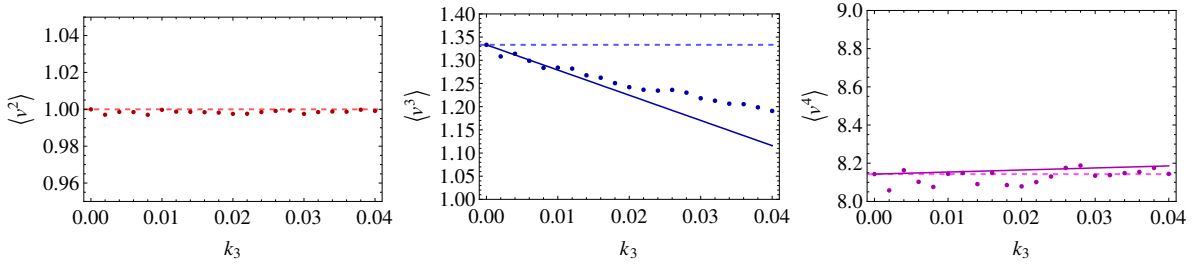


FIG. 2. Comparison between statistical moments of the velocity versus the non-linear constant  $k_3$  for a system with  $\lambda = 1$ ,  $\Phi = 1$ ,  $k_1 = 1$  and  $m = 1$ . The symbols are obtained from averages over  $10^7$  numerical realisations and the dashed lines correspond to our first order calculations as provided in the main text and the EPAPS. The full lines correspond to the respective first order approximation and dashed horizontal lines point the linear case value:  $\langle v^2 \rangle = 1$ ,  $\langle v^3 \rangle = 4/3$  and  $\langle v^4 \rangle = 57/7$ .

Equation (19) is equal to that we computed for the Gaussian reservoir [16]. Moreover, higher non-linear orders in  $k_3$  of  $\overline{v^2_{nl}}$  zero out as well (see numerical corroboration in the left panel of Fig. 2 and the analytics in the EPAPS Appendix C). Nonetheless, the introduction of non-linearities in an athermal system modifies the distribution of the velocities, in opposition to the thermal case. That is clear from the numerical analysis of the model shown in Figs. 2 and 3.<sup>3</sup>

According to what we said, the average kinetic energy always reads,

$$\begin{aligned} \mathcal{K} &\equiv \frac{1}{2}m\overline{v^2} \\ &= \frac{1}{4}\frac{\lambda}{\gamma}\langle \Phi^2 \rangle = \frac{1}{2}T, \end{aligned} \quad (20)$$

<sup>2</sup> The path of integration used for determination of time independent quantities is plotted in Fig. 1 of the EPAPS [22].

<sup>3</sup> The numerical implementation of our model corresponds to the second method introduced in the appendix of Ref. [17].

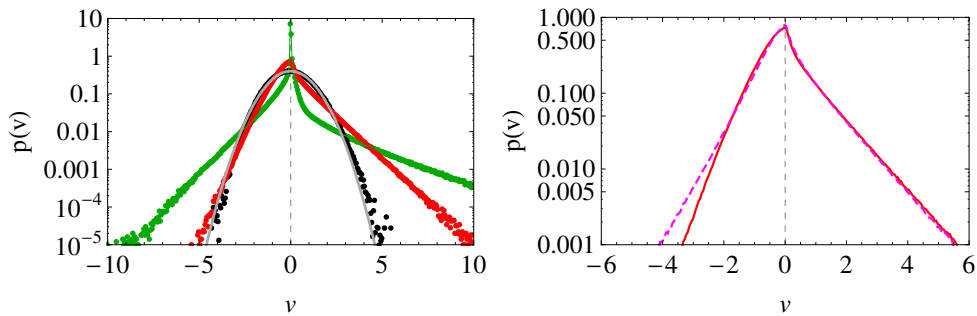


FIG. 3. Probability density function of the velocity  $p(v)$  versus velocity  $v$  (in log-linear scale) obtained from numerical simulation with parameters  $k_1 = 1$ ,  $k_3 = 0$  and  $m = 1$  and  $T = 1$  for an exponentially distributed shot-noise amplitude. Left panel:  $k_1 = 1$ ,  $k_3 = 0$  and  $\lambda = 1/10$  (green symbols),  $\lambda = 1$  (red symbols),  $\lambda = 100$  (black symbols). The grey line the a Gaussian with variance equal to one which is the thermal limit. Right panel:  $\lambda = 1$ ,  $k_1 = 1$ ,  $k_3 = 0$  for the full red line and  $k_3 = 1/5$  for the magenta dashed line showing that  $p(v)$  is sensitive to  $k_3$ .

where,

$$T \equiv \frac{1}{2} \frac{\lambda}{\gamma} \langle \Phi^2 \rangle. \quad (21)$$

independently of the non-linearity. In other words, we resort to the canonical definition of temperature to define the effective temperature — which is not the standard thermal quantity — of this non-equilibrium system by means of an expression [Eq. (21)] that resembles the thermal fluctuation-dissipation relation.

That relation throws light on the implications of a Poissonian shot-noise reservoir; let us fix the canonical temperature of the system at  $T$  and let us modify the rate of interaction between the particle and the medium,  $\lambda$ . In the limit  $\lambda \rightarrow \infty$ , we can observe that the distribution of the velocities converges to the Gaussian. Looking at Eq. (15), it is visible that,

$$\overline{\overline{v^n}} \propto \lambda \langle \Phi^n \rangle. \quad (22)$$

Using Jensen's inequality, particularly,  $|\langle \Phi^n \rangle| \leq \langle \Phi^2 \rangle^{n/2}$ , we have,

$$\overline{\overline{v^n}} \lesssim \lambda \langle \Phi^2 \rangle^{n/2} = \lambda \left( \frac{2\gamma T}{\lambda} \right)^{n/2} \quad (23)$$

$$\lim_{\lambda \rightarrow \infty} \overline{\overline{v^n}} \sim \lambda^{1-n/2} = 0, \quad (n \geq 3),$$

which confirms the Gaussian limit. For the position, similar considerations will apply in the linear case. The difference between them relies on the fact that the average of the position is not necessarily equal to zero, as it must be for the velocity. Therefore, only when the noise is symmetrical, the continuous noise limit ( $\lambda \rightarrow \infty$ ) yields the Boltzmann-Gibbs result,

$$p(x) = \frac{1}{Z_x} \exp \left[ -\frac{1}{2T} \left( k_1 x^2 + \frac{1}{2} k_3 x^4 \right) \right]. \quad (24)$$

Concomitantly, in Fig. 4 we show the distribution of the position,  $p(x)$ , obtained from numerical simulation for two situations with the same canonical amplitude,  $T = 1$ ; on the left panel the amplitude is exponentially distributed and on the right panel a Gaussian.

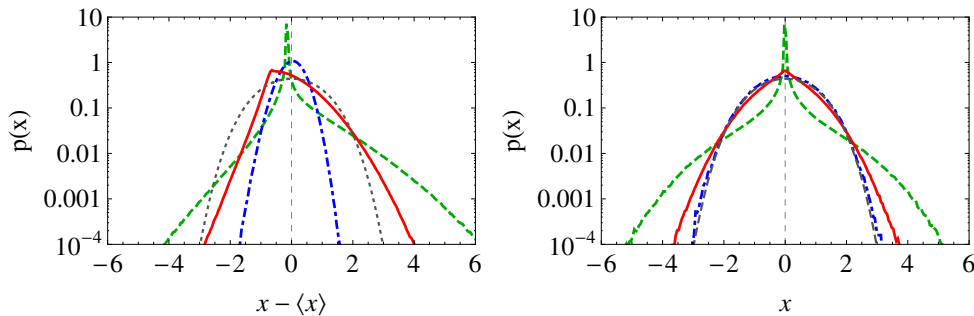


FIG. 4. Probability density function of the position  $p(x)$  versus position  $x$  (in log-linear scale) obtained from numerical simulation with parameters  $k_1 = 1$ ,  $k_3 = 0$  and  $m = 1$  and  $T = 1$ . On the left panel  $\Phi$  is exponentially distributed — and thus we have an average value  $\langle x \rangle \neq 0$  — whereas on the right panel  $\Phi$  is Gaussian distributed. The legend goes as follows:  $\lambda = 1/10$  (green dashed line),  $\lambda = 1$  (red full line),  $\lambda = 100$  (blue dot-dashed line). The grey dashed line corresponds to Eq. (24) for these parameters. The green dashed curve resembles stationary distributions that can be found in granular matter problems as well [24].

This account perfectly fits the problem of the Andersen thermostat [11] that we will treat from a first principles in a forthcoming paper. In general terms, it corresponds to a reservoir in the form of a little dense medium so that the number of collisions in an infinitesimal time interval is not enough for a worthwhile assumption of the central limit theorem. The problem as it stands yields a mean free path for the Poissonian particle of

the order of,

$$\ell = \sqrt{\frac{T}{m \lambda^2}}. \quad (25)$$

Under these conditions the reservoir is athermally internal, *i.e.*, the dissipation effect is an intrinsic trait of the medium and cannot be dissociated from the fluctuations. This framework is close to the granular gas picture for shot-noise recently published in Ref. [14] as well. On the other hand, that is quite different from the perspective of a molecular motor powered by exergonic chemical reactions such as kinesin motion on actin microtubules, which is another frequent example of a system subject to a shot-noise reservoir [9]. Therein, because the dissipation and the fluctuations have different origins, the athermal reservoir is actually an external work reservoir, even if fluctuation and dissipation spectra match.

## B. Potential energy

### 1. Linear contribution

The average potential energy of our non-linear system is defined as,

$$\begin{aligned} \mathcal{V} &= \frac{1}{2} k_1 \overline{x^2} + \frac{1}{4} k_3 \overline{x^4} \\ &= \mathcal{V}_2 + \mathcal{V}_4. \end{aligned} \quad (26)$$

From Eq. (8), the non-linear  $n^{\text{th}}$ -order moment of the position is given by,

$$\begin{aligned} \overline{x^n} &= \lim_{z, \epsilon \rightarrow 0} \int_{-\infty}^{\infty} \prod_{j=1}^n \frac{dq_j}{2\pi} \frac{z}{z - \sum_{l=1}^n (i q_l + \epsilon)} \times \left\langle \prod_{i=1}^n \frac{\tilde{\eta}(i q_i + \epsilon)}{R(i q_i + \epsilon)} - k_3 \prod_{i=1}^n \frac{1}{R(i q_i + \epsilon)} \right. \\ &\quad \left. \times \lim_{\epsilon \rightarrow 0^+} \int \prod_{j=1}^3 \frac{dq_{ij}}{2\pi} \left[ i q_i + \epsilon - \sum_{j=1}^3 (i q_{ij} + \epsilon) \right]^{-1} \prod_{l=1}^3 \frac{\tilde{\eta}(i q_{il} + \epsilon)}{R(i q_{il} + \epsilon)} + O(k_3^2) \right\rangle, \end{aligned} \quad (27)$$

where we can separate out the linear contribution,

$$\overline{x^n}_1 = \lim_{z, \epsilon \rightarrow 0} \int_{-\infty}^{\infty} \prod_{j=1}^n \frac{dq_j}{2\pi} \frac{z}{z - \sum_{l=1}^n (i q_l + \epsilon)} \left\langle \prod_{i=1}^n \frac{\tilde{\eta}(i q_i + \epsilon)}{R(i q_i + \epsilon)} \right\rangle, \quad (28)$$

and non-linear counterpart, which in first order of  $k_3$ , equals,

$$\begin{aligned} \overline{x}_{\text{nl}}^n = & -n k_3 \lim_{z, \epsilon \rightarrow 0} \int_{-\infty}^{\infty} \prod_{i=1}^n \frac{dq_i}{2\pi} \frac{z}{z - \sum_{j=1}^n (i q_j + \epsilon)} \frac{1}{R(i q_i + \epsilon)} \times \\ & \int \prod_{j=1}^3 \frac{dq_{1,j}}{2\pi} \frac{1}{i q_1 + \epsilon - \sum_{j=1}^3 (i q_{1,j} + \epsilon)} \left\langle \prod_{l=2}^n \tilde{\eta}(i q_l + \epsilon) \prod_{j=1}^3 \frac{\tilde{\eta}(i q_{1,j} + \epsilon)}{R(i q_{1,j} + \epsilon)} \right\rangle + O(k_3^2). \end{aligned} \quad (29)$$

For the linear part, employing Eq. (13), we have,

$$\begin{aligned} \overline{x}_1^2 = & \overline{\overline{x}}_1^2 + \overline{\overline{x}}_1^2 \\ & = \frac{\lambda \langle \Phi^2 \rangle}{2 \gamma k_1} + \left( \frac{\lambda \langle \Phi \rangle}{k_1} \right)^2, \end{aligned} \quad (30)$$

where the second term on the right-hand side appears because of the non-zero average position,

$$\overline{\overline{x}}_1 = \frac{\lambda \langle \Phi \rangle}{k_1}, \quad (31)$$

if the stochastic term has  $\langle \Phi \rangle \neq 0$ .<sup>4</sup> Because the minimum of the potential does not coincide with the average position there is a energetic cost to the system equal to,

$$\mathcal{E}_0 = \frac{1}{2} k_1 \overline{\overline{x}}_1^2 = \frac{\lambda^2 \langle \Phi \rangle^2}{2 k_1}, \quad (32)$$

that could be assumed as the ground energy. With that shift and taking into consideration the value of the canonical temperature Eq. (21), if we take the limit  $k_3 \rightarrow 0$ , equipartition of energy arises

$$\mathcal{V}_2 = \frac{1}{2} T, \quad (33)$$

and we get,

$$T = \frac{\lambda \langle \Phi^2 \rangle}{2 \gamma}, \quad (34)$$

which is exactly the same relation as obtained from the calculations for the kinetic energy Eq. (21). That equality props up the use of the concept of temperature even though we are treating an athermal system.

---

<sup>4</sup> This situation is unnatural for a internal shot-noise reservoir, but is quite likely for work shot-noise reservoirs [9].

## 2. Non-linear terms

As we have verified and reasoned on, the non-linear nature of the potential does not affect the two first order moments of the velocity, which is not the case for the potential energy. In Eq. (13), we have provided a way of computing the cumulants of the position in the linear case and whence any moment of the potential energy is obtained with little effort. However, calculations for a non-linear system in contact with a non-Gaussian reservoir are far more complex. First, the evaluation of each  $\overline{x^n_{\text{nl}}}$  calls for determining an ever larger number of terms because the Isserlis-Wick theorem — that is so useful for Gaussian reservoir calculations — cannot be used; second, when the system is non-linear, one cannot add the cumulants of the linear and non-linear contributions because the cumulants do not benefit from the superposition property. Despite its complexity and inspired by a diagrammatic representation, we were capable of establishing a *modus calculandi* that allows writing the first order contribution of any statistical moment of the position in terms of zeroes  $\zeta_{\pm}$ . For the purpose of conciseness of the core text, we present the method in Appendix A.

The introduction of the non-linearity,  $k_3 \neq 0$ , directly affects  $\mathcal{V}_2$ , so that,

$$\begin{aligned} \mathcal{V}_2 &= \mathcal{V}_1 + \mathcal{V}_{2,\text{nl}} \\ &= \frac{1}{2}k_1\overline{x^2_1} + \frac{1}{2}k_1\overline{x^2_{\text{nl}}}. \end{aligned} \tag{35}$$

For more details, see our calculations [22].

With respect to the direct anharmonic contribution to the potential energy we have  $\mathcal{V}_4 = \frac{1}{4}k_3\overline{x^4}$ . Keeping only up to first order, we just need to apply the standard relation between moments and cumulants,

$$\mathcal{V}_4 = \frac{1}{4}k_3 \sum_{i=0}^4 \mathcal{C}_i^4 \overline{x^{4-i}} \overline{x^i}, \tag{37}$$

where  $\mathcal{C}_i^4$  are the coefficients that link the fourth-order cumulant and fourth-order moments [26]. Therefrom, we can obtain the nonlinear potential energy [22].

Note that in the case  $\langle \Phi \rangle = 0$  and in the limit  $\lambda \rightarrow \infty$  (and temperature fixed), all the terms vanish but the third,  $\left(\frac{\lambda \langle \Phi^2 \rangle}{2\gamma k_1}\right)^2$ . As provided by Eq. (34), that term is the (square)

temperature and thus the non-linear contribution in the Gaussian case of Paper I,

$$\lim_{\lambda \rightarrow \infty} \mathcal{V}_{\text{nl}}|_T = -\frac{3 k_3}{4 k_1^2} T^2, \quad (38)$$

is retrieved in that limit.

Taking into account Eq. (29), the average value of the position is also modified by,<sup>5</sup>

$$\begin{aligned} \bar{x}_{\text{nl}} &= -k_3 \left[ \frac{2 \lambda \langle \Phi^3 \rangle}{3 k_1^3 m + 6 k_1^2 \gamma^2} + 3 \frac{\lambda^2 \langle \Phi \rangle \langle \Phi^2 \rangle}{2 k_1^3 \gamma} + \frac{\lambda^3 \langle \Phi \rangle^3}{k_1^4} \right] + O(k_3^2). \\ &= -\frac{k_3}{k_1} \left[ \overline{x^3} + 3 \overline{x^2 \bar{x}} + \bar{x}^3 \right] + O(k_3^2) \end{aligned} \quad (39)$$

Equation (39) tells us that only when the reservoir is symmetrical (*e.g.*, a heat reservoir) there is no contribution from the non-linearities to the average position. Moreover, it suggests that, by honinng the non-linear constant  $k_3$ , it could be possible to make  $\bar{x} = 0$ . Nevertheless, either from higher-order calculations or numerical analysis, we verify that although  $\bar{x}$  decreases with increasing  $k_3$ , the value of the average position only vanishes in the limit  $k_3 \rightarrow \infty$ .

There is a connection between the effect of  $\bar{x}$  approaching the origin and the diminishing of  $\overline{v^3}$  with  $k_3$ . As we augment  $k_3$ , we lessen  $\bar{x}$ ; in doing that, we allow the particle to swing more equally between both sides, *i.e.*, to have larger negative values of the velocity, a behaviour that makes the asymmetry of  $p(v)$  — and its proxy  $\overline{v^3}$  — smaller.

In Fig. 5, we present a comparison between the first four statistical moments of the position given by our first order calculations (lines) and the values obtained from numerical realisations and in Fig. 6 the relative error between analytical approximation and numerical results. The goodness of the approximation can be further improved by computing higher order terms in  $k_3$ , as we show with the dot-dashed line representing the addition of the second order contribution for the average value with its analytical expressions presented in the EPAPS.

We now recall prior results of us regarding the heat flux between particles in contact with non-Gaussian athermal reservoirs. As we stated in Ref. [15], by introducing non-linearities in the system, we call down the higher-order cumulants of  $\eta$  in our calculations,

---

<sup>5</sup> Since we are only considering first order non-linear contributions the following term is ignored for the calculations of  $\mathcal{V}$ .

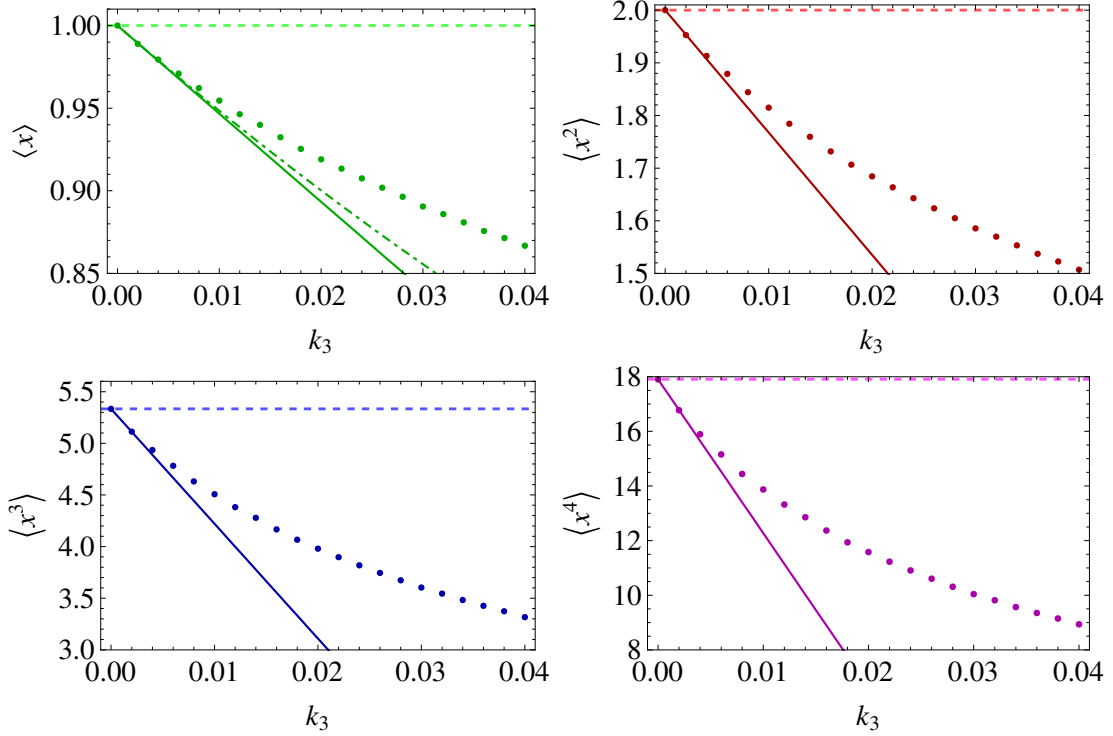


FIG. 5. Comparison between statistical moments of the position versus the non-linear constant  $k_3$  for a system with  $\lambda = 1$ ,  $\Phi = 1$ ,  $k_1 = 1$  and  $m = 1$ . The symbols are obtained from averages over  $10^7$  numerical realisations and the lines correspond to our first order calculations as provided in the main text and the EPAPS. The dashed horizontal lines point the linear values:  $\langle x \rangle = 1$ ,  $\langle x^2 \rangle = 1$ ,  $\langle x^3 \rangle = 16/3$  and  $\langle x^4 \rangle = 376/21$ . The dot-dashed line corresponds to the approximation up to second order we make explicit in the EPAPS as well.

which — in terms of physical properties — can be “*understood as higher-order sources of energy*” that change the value of  $\mathcal{V}$  in comparison with Gaussian reservoirs.<sup>6</sup> By analogy with the relation established between the second order cumulant of velocity — as well as the position in the linear case — and the canonical temperature, we define a  $n$ -th order temperature as a quantity proportional to the  $n$ -th order cumulant

$$\mathcal{T}_n \equiv k_1^{n/2} \overline{x_1^n}, \quad (40)$$

where  $\mathcal{T}_2 = T$ .

<sup>6</sup> Taking into consideration we are making a first order analysis it is important to recall that we are talking about an infinite set of reservoirs, each corresponding to a given order of the cumulant of the noise.

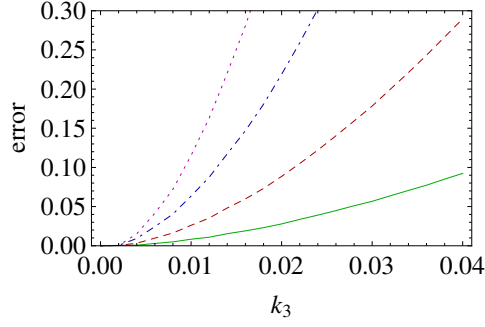


FIG. 6. Relative error,  $\text{error} = \left| \frac{\langle x_{\text{analytical}}^n \rangle - \langle x_{\text{numerical}}^n \rangle}{\langle x_{\text{numerical}}^n \rangle} \right|$ , of the first order approximation of the statistical moments and the analytical approximation for the same parameters used in Fig. 5. The colours follow the same scheme as previously presented: full green line ( $\langle x \rangle$ ), dashed red line ( $\langle x^2 \rangle$ ), dot-dashed blue line ( $\langle x^3 \rangle$ ) and dotted magenta line ( $\langle x^4 \rangle$ ). Naturally, as the order of the statistical moment increases the series expansion requires further order in  $k_3$ .

For a general form of the noise, its cumulants may be given by

$$\overline{\overline{\tilde{\eta}(s_1)\tilde{\eta}(s_2)\dots\tilde{\eta}(s_n)}}} = \frac{\phi_{n,c}}{\sum_{j=1}^n s_j}, \quad (41)$$

where  $\phi_{n,c}$  stands for the  $n$ -th order cumulant of the noise. Thus, in the limit  $k_3 \rightarrow 0$ , we can write explicitly

$$\begin{aligned} \mathcal{T}_n &= k_1^{n/2} \lim_{z \rightarrow 0} \lim_{\epsilon \rightarrow 0} \int_{-\infty}^{\infty} \prod_{b=1}^n \frac{dq_b}{2\pi} \frac{z}{z - \sum_{b=1}^n (iq_b + \epsilon)} \frac{\overline{\overline{\prod_{b=1}^n \tilde{\eta}(iq_b + \epsilon)}}}{\overline{\overline{\prod_{b=1}^n R(iq_b + \epsilon)}}} \\ &= k_1^{n/2} \phi_{n,c} \lim_{z \rightarrow 0} \lim_{\epsilon \rightarrow 0} \int_{-\infty}^{\infty} \prod_{b=1}^n \frac{dq_b}{2\pi} \frac{z}{z - \sum_{b=1}^n (iq_b + \epsilon)} \frac{1}{\overline{\overline{\prod_{b=1}^n R(iq_b + \epsilon)}}} \frac{1}{\sum_{j=1}^n (iq_j + \epsilon)} \\ &\propto \phi_{n,c}. \end{aligned} \quad (42)$$

Observe that is, in this case, exactly proportional to the corresponding cumulant of the noise. When non-linearities are present, the above contribution to  $\mathcal{T}_n$  is still present as the lowest order term in an expansion on orders of  $k_3$ .

Definition (40) can be extended to the standard thermal reservoir. In that case the noise distribution is Gaussian and hence any cumulant other than the second is equal to zero as well as the higher-order temperatures ( $n \neq 0$ ). Applying Eq. (40), we write the

non-linear potential energy as,

$$\mathcal{V}_{\text{nl}} = -\frac{3 k_3}{4 k_1^2} \left[ \frac{1}{3} \mathcal{T}_4 + 2 \mathcal{T}_3 \mathcal{T}_1 + \mathcal{T}_2^2 + 2 \mathcal{T}_2 \mathcal{T}_1^2 + \mathcal{T}_1^4 \right], \quad (43)$$

and the energy (after removing  $\mathcal{E}_0$ ),

$$\mathcal{E} = \mathcal{T}_2 - \frac{3 k_3}{4 k_1^2} \left[ \frac{1}{3} \mathcal{T}_4 + 2 \mathcal{T}_3 \mathcal{T}_1 + \mathcal{T}_2^2 + 2 \mathcal{T}_2 \mathcal{T}_1^2 + \mathcal{T}_1^4 \right]. \quad (44)$$

### C. Thermostatistical response functions

In this sub-section, we analyse how the (average) energy of the system responds to changes in the parameters of the problem. First, we analyse the specific heat of the system,

$$\nu \equiv \frac{\partial \mathcal{E}}{\partial T} = \frac{\partial \mathcal{E}}{\partial \mathcal{T}_2} = 1 - \frac{3 k_3}{2 k_1^2} (\mathcal{T}_2 + \mathcal{T}_1^2) + O \left( \left[ \frac{k_3 \mathcal{T}_2}{k_1^2} \right]^2 \right). \quad (45)$$

This expression is close to the relation for the Gaussian case, except the term coming from the first order cumulant that is typical of a work reservoir. Let us now take into consideration definition Eq. (40); note that each cumulant  $\overline{x_1^n}$  does only involve the  $n$ -th order cumulant of the noise, a quantity that we assumed as a mathematical representation higher-order energy sources. Accordingly, we assess the sensitivity of the energy of the system to changes in those sources by defining the  $n$ -th order specific heat,

$$\nu_n \equiv \frac{\partial \mathcal{E}}{\partial \mathcal{T}_n}. \quad (46)$$

In first order of  $k_3$ , we have,

$$\begin{aligned} \nu_1 &= \frac{\partial \mathcal{E}}{\partial \mathcal{T}_1} = -3 \frac{k_3}{k_1^2} \left( \mathcal{T}_1^3 + \mathcal{T}_2^2 \mathcal{T}_1 + \frac{1}{2} \mathcal{T}_3 \right) + \dots \\ \nu_3 &= \frac{\partial \mathcal{E}}{\partial \mathcal{T}_3} = -\frac{3 k_3}{2 k_1^2} \mathcal{T}_1 + \dots \\ \nu_4 &= \frac{\partial \mathcal{E}}{\partial \mathcal{T}_4} = -\frac{1 k_3}{4 k_1^2} + \dots \end{aligned} \quad (47)$$

Equation (47) shows that these higher-order response functions are only different from zero when the system is non-linear and thus we have the higher-order sources of energy acting upon the system. Furthermore, in having established a given canonical temperature, we verify that only when the system becomes non-linear there is an explicit dependence of the average energy with the mechanical parameters of the system  $k_1$ ,  $k_3$ ,  $\gamma$  and  $m$ . As a matter

of fact, our result clearly puts into the limelight the connection between the mechanical properties of a system and the activation or idleness of the higher-order energy sources of a singular measure reservoir.

From the variance of the position,

$$\begin{aligned}\sigma_x^2 &\equiv \langle x^2 \rangle - \langle x \rangle^2 \\ &= \frac{\mathcal{T}_2}{k_1} - 3 \frac{k_3}{k_1^3} \left( \frac{1}{3} \mathcal{T}_4 + \mathcal{T}_3 \mathcal{T}_1 + \mathcal{T}_2^2 + \frac{1}{2} T \mathcal{T}_1^2 \right) + O(k_3^2)\end{aligned}\quad (48)$$

we define a generic coefficient of displacement,

$$\alpha_n \equiv \frac{1}{\sigma_x^2} \frac{\partial \sigma_x^2}{\partial \mathcal{T}_n}.$$
 (49)

For the canonical temperature we obtain,

$$\alpha \equiv \alpha_2 = \frac{1}{\mathcal{T}_2} + 3 \frac{k_3}{k_1^2} \left( 1 + \frac{\mathcal{T}_3 \mathcal{T}_1}{\mathcal{T}_2^2} + \frac{\mathcal{T}_4}{3 \mathcal{T}_2^2} \right) + O(k_3^2),$$
 (50)

that is different from the Gaussian reservoir case, even when the reservoir is mathematically described by a symmetric noise. With respect to non-linear displacement coefficients in first order they read,

$$\begin{aligned}\alpha_1 &= -3 \frac{k_3}{k_1^2} \left( \mathcal{T}_1 + \frac{\mathcal{T}_3}{\mathcal{T}_2} \right), \\ \alpha_3 &= -3 \frac{k_3}{k_1^2} \frac{\mathcal{T}_1}{\mathcal{T}_2}, \\ \alpha_4 &= -\frac{k_3}{k_1^2} \frac{1}{\mathcal{T}_2}.\end{aligned}\quad (51)$$

In the high rate limit, we have  $\alpha_n = 0$  (for all  $n \neq 2$ ) and  $\alpha = \mathcal{T}_2^{-1} + 3k_3/k_1^2$ . In all higher-order cases, we find, without surprise, that by stiffening the spring the displacement features of the system diminish. Because the average position is different from zero when the shot-noise is one-side distributed, we further introduce an extended definition of the thermal expansion of the system,

$$\beta_n \equiv \frac{1}{\bar{x}} \frac{\partial \bar{x}}{\partial \mathcal{T}_n},$$
 (52)

which give the explicit expressions,

$$\begin{aligned}\beta_1 &= \frac{1}{\mathcal{T}_1} \left( 1 + \frac{k_3}{k_1^2} \frac{\mathcal{T}_3 - 2\mathcal{T}_1^3}{\mathcal{T}_1} \right), \\ \beta_2 &= -3 \frac{k_3}{k_1^2} \\ \beta_3 &= -3 \frac{k_3}{k_1^2} \frac{1}{\mathcal{T}_1}.\end{aligned}\tag{53}$$

#### IV. HEAT FLUX ANALYSIS

The total average energy,  $\mathcal{E} = \mathcal{K} + \mathcal{V}_2 + \mathcal{V}_{nl}$ , results from the superposition of the fluxes describing the total injected energy,

$$J(\Xi) \equiv \int_0^\Xi \eta(t) v(t) dt,\tag{54}$$

and the total dissipated energy,

$$D(\Xi) \equiv -\gamma \int_0^\Xi v(t)^2 dt.\tag{55}$$

Herein, we concentrate our effort on understanding both long-term behaviour. Bearing in mind the results for the dependence of  $p(v)$  from  $k_3$ , the non-linearity will also change the statistics of the fluxes. This constitutes an important difference between (shot-noise) athermal and thermal reservoirs. It must be stressed that for thermal reservoirs only the memory features and the initial conditions [27] of the bath have an impact on the statistics of the fluxes. In this section, we restrict ourselves to the linear situation because to the best of our knowledge such results are absent in the literature. Moreover, it is worth noticing that an analysis of the athermal linear case is already tricky.

For large  $\Xi \gg \theta^{-1} = m/\gamma$ , the average inject flux reads,

$$\begin{aligned}\langle J(\Xi) \rangle &\asymp \lim_{\epsilon \rightarrow 0} \int_0^\Xi dt \prod_{j=1}^2 \int_{-\infty}^{\infty} \frac{dq_j}{2\pi} e^{(iq_1 + iq_2 + 2\epsilon)t} (iq_2 + \epsilon) \left\langle \tilde{\eta}(iq_1 + \epsilon) \frac{\tilde{\eta}(iq_2 + \epsilon)}{R(iq_2 + \epsilon)} \right\rangle \\ &= \frac{\lambda \langle \Phi^2 \rangle}{2m} \Xi.\end{aligned}\tag{56}$$

The average dissipated heat,

$$\langle D(\Xi) \rangle \asymp -\gamma \lim_{\epsilon \rightarrow 0} \int_0^\Xi dt \int_{-\infty}^{\infty} \prod_{j=1}^2 \frac{dq_j}{2\pi} e^{(iq_1 + iq_2 + 2\epsilon)t} \left\langle \prod_{i=1}^2 (iq_i + \epsilon) \frac{\tilde{\eta}(iq_i + \epsilon)}{R(iq_i + \epsilon)} \right\rangle\tag{57}$$

has a constant part,

$$\begin{aligned} \langle D(\Xi \gg m/\gamma) \rangle_0 = & \frac{1}{2} \left[ \frac{\lambda \langle \Phi^2 \rangle}{\gamma} + \frac{\lambda^2 \langle \Phi \rangle^2}{k_1} \right] - \frac{3 k_3}{4 k_1} \left( \frac{\lambda \langle \Phi^4 \rangle}{4 \gamma (4 m k_1 + 3 \gamma^2)} + \frac{4 \lambda^2 \langle \Phi^3 \rangle \langle \Phi \rangle}{3 k_1 (m k_1 + 2 \gamma^2)} \right. \\ & \left. + \frac{\lambda^2 \langle \Phi^2 \rangle^2}{4 \gamma^2 k_1} + \frac{2 \lambda^3 \langle \Phi^2 \rangle \langle \Phi \rangle^2}{\gamma k_1^2} + \frac{\lambda^4 \langle \Phi \rangle^4}{k_1^3} \right) + O(k_3^2) = \mathcal{E} \end{aligned}$$

that equals the average energy of the system and a linearly time dependent contribution,

$$\langle D(\Xi) \rangle \asymp -\frac{\lambda \langle \Phi^2 \rangle}{2 m} \Xi, \quad (58)$$

that assures that the overall entropy production sets off as it must be for a steady state. It is easy to understand that the average value of the fluxes is the only statistical moment that is not influenced by  $k_3$ . One just needs to remind that the long-term second-order moment of the velocity is independent of the form of the potential. The remaining moments and consequently the distribution are  $k_3$  dependent.

### A. Large Deviation Analysis of the fluxes

We carry on our analysis by computing the asymptotic cumulants of the fluxes,

$$\langle\langle \mathcal{J}^n \rangle\rangle \equiv \Xi \lim_{t \rightarrow \infty} \frac{1}{t} \langle\langle J(t)^n \rangle\rangle, \quad (59)$$

that yield the same result for absolute values of the injected and dissipated fluxes. Since the Poissonian problem implies the systematic use of the cumulants of the noise, we compute the cumulants of  $\langle\langle \mathcal{J}^n \rangle\rangle$  using the equation for the dissipated flux,

$$\langle D(\Xi)^n \rangle = (-\gamma)^n \left\langle \prod_{l=1}^n \int_0^\Xi dt_l \prod_{j=1}^2 \int_{-\infty}^{\infty} \frac{dq_{jl}}{2\pi} e^{(iq_{1l} + iq_{2l} + 2\epsilon)t_l} (iq_{1l} + \epsilon)(iq_{2l} + \epsilon) \frac{\tilde{\eta}(iq_{1l} + \epsilon)}{R(iq_{1l} + \epsilon)} \frac{\tilde{\eta}(iq_{2l} + \epsilon)}{R(iq_{2l} + \epsilon)} \right\rangle \quad (60)$$

which bears a larger number of symmetries that make the full calculation simpler and faster.

Recalling that Poisson noise is defined in terms of its cumulants, we must rewrite the moments of the fluxes in a cumulant form. We address the reader to the EPAPS for the entire calculation and restrict ourselves to the results of the first four cumulants of the energy fluxes. They read, for the second,

$$\langle\langle \mathcal{J}^2 \rangle\rangle = \frac{\lambda \langle \Phi^4 \rangle}{4 m^2} \Xi + 2 \frac{\lambda^2 \langle \Phi^2 \rangle^2}{4 m \gamma} \Xi, \quad (61)$$

for the third,

$$\begin{aligned} |\langle\langle \mathcal{J}^3 \rangle\rangle| &= \frac{\lambda \langle \Phi^6 \rangle}{8 m^3} \Xi + \frac{3 \lambda^2 \langle \Phi^2 \rangle \langle \Phi^4 \rangle}{2 m^2} \Xi \\ &+ \frac{2 \gamma \lambda^2 \langle \Phi^3 \rangle^2}{3 m^2 (2\gamma^2 + k m)} \Xi + \frac{3 \lambda^3 \langle \Phi^2 \rangle^3}{2 m \gamma^2} \end{aligned} \quad (62)$$

and for the fourth,

$$\begin{aligned} \langle\langle \mathcal{J}^4 \rangle\rangle &= \frac{\lambda \langle \Phi^8 \rangle}{16 m^4} \Xi + \frac{3 \lambda^2 \langle \Phi^2 \rangle \langle \Phi^6 \rangle}{2 m^3 \gamma} \Xi + \frac{8 \gamma \lambda^2 \langle \Phi^3 \rangle \langle \Phi^5 \rangle}{3 m^3 (2\gamma^2 + k m)} + \frac{3 \lambda^2 \langle \Phi^4 \rangle^2}{2 m^3 \gamma} \Xi \\ &+ 12 \frac{\lambda^3 \langle \Phi^2 \rangle^2 \langle \Phi^4 \rangle}{m^2 \gamma^2} \Xi + \frac{16 \lambda^3 (4\gamma^2 + k m) \langle \Phi^2 \rangle \langle \Phi^3 \rangle^2}{3 m^2 (2\gamma^2 + k m)^2} + \frac{15 \lambda^4 \langle \Phi^2 \rangle^4}{2 m \gamma^3}. \end{aligned} \quad (63)$$

In Fig. 7, we present the time evolution of the cumulants of the flux  $\mathcal{J}$  where is clear the emergence of the asymptotic regime of Eqs. (56), (61)-(63). From these cumulants, we compute the limit distributions depending on the rate of kicks. When  $\lambda \ll 1$ , we have a lower bound limit to our problem. In this case, the leading contribution comes from the term proportional to  $\lambda$  that appears in the cumulant  $\langle\langle \mathcal{J}^n \rangle\rangle$ . This means that from Eqs. (61)-(63) we induce,

$$\lim_{\lambda \ll 1} \langle\langle \mathcal{J}^n \rangle\rangle = \lambda \frac{\langle \Phi^{2n} \rangle}{2^n m^n} \Xi. \quad (64)$$

For a Gaussian shot-noise amplitude,  $\Phi$ , the cumulants of the fluxes become,

$$\lim_{\lambda \ll 1} \langle\langle \mathcal{J} (\Xi)^n \rangle\rangle|_{\text{Gauss}} = \lambda \frac{\sigma^{2n} (2n-1)!!}{2^n m^n} \Xi, \quad (65)$$

that give the cumulant generating function,

$$\mathcal{G}_{\mathcal{J}}^{(l)}(\varphi) \Big|_{\text{Gauss}} = \lambda \Xi \left( \frac{m}{\sqrt{m(m - \sigma^2 \varphi)}} - 1 \right), \quad (66)$$

where  $\mathcal{G}_{\mathcal{J}}^{(l)}(0) \Big|_{\text{Gauss}} = 0$ . Using a Legendre Transform according to the Gärtner-Ellis Theorem [28], the inversion yields,<sup>7</sup>

$$\mathcal{L}^{(l)}(\mathcal{J}) \Big|_{\text{Gauss}} \sim \exp \left[ -\mathcal{J} / \langle \mathcal{J} \rangle + (\mathcal{J} / \langle \mathcal{J} \rangle)^{1/3} \right] \Theta(\mathcal{J}), \quad (67)$$

where according to Eq. (65),  $\langle \mathcal{J} \rangle = \frac{\lambda \sigma^2 \Xi}{2m}$ .

<sup>7</sup> For exponentially distributed amplitudes, we found that  $\sum_{n=1}^{\infty} \langle\langle \mathcal{J}^n \rangle\rangle \varphi^n / n!$  does not converge because the term  $(2n)!$  that appears in the numerator for this case grows faster than  $n!$ .

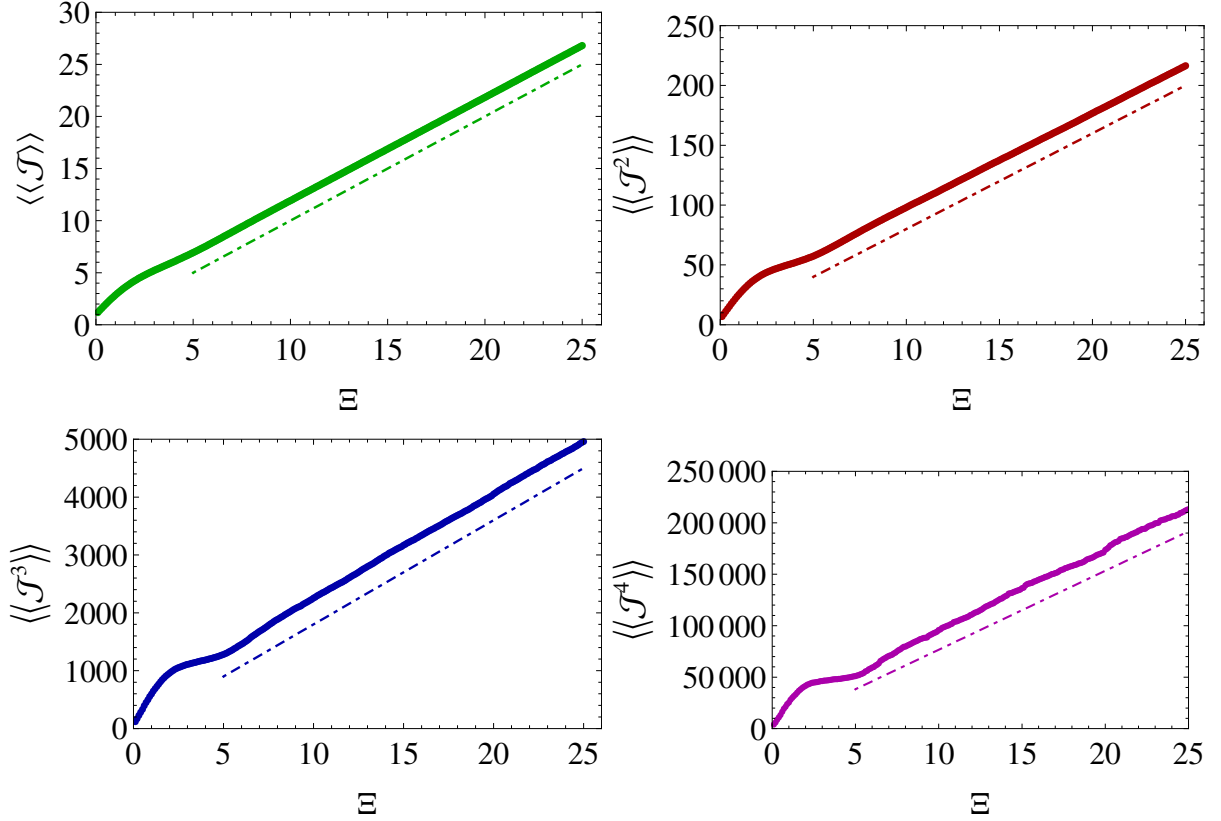


FIG. 7. Time evolution of the first four order cumulants of the flux  $|\langle\langle \mathcal{J}^n \rangle\rangle|$  obtained by numerical simulation of a exponentially distributed shot-noise with all parameters equal to 1 but  $k_3 = 0$ . The dot-dashed lines correspond to the straight lines which have the same slope of the long-term evolution. They are equal to: 1, 8, 180 and  $23008/3$ , respectively.

On the other hand, when the rate is very high,  $\lambda \gg 1$ , we have the lower bound of the problem. The cumulants are dominated by the last term proportional to  $\lambda^n \langle \Phi^2 \rangle^n$  and we reobtain the formula of a Gaussian white noise reservoir,

$$\mathcal{G}_{\mathcal{J}}^{(u)}(\varphi) = \frac{\gamma \Xi}{2m} \left( 1 - \sqrt{1 + 4T\varphi} \right), \quad (68)$$

which corresponds to well-known thermal the large deviation function,

$$\mathcal{L}^{(u)}(\mathcal{J}) = \frac{1}{\mathcal{N}} \exp \left[ -\frac{(\mathcal{J} - \frac{\gamma m}{T} \Xi)^2}{4T\mathcal{J}} \right] \Theta[\mathcal{J}], \quad (69)$$

already found in previous works employing different methodologies [16, 29].<sup>8</sup> In Fig. 8,

<sup>8</sup> Reference [29] shows numerically that the large deviation function of the fluxes does not depend on

we show  $\mathcal{L}(\mathcal{J})$  for different values of  $\lambda$  and the same canonical temperature including the approach to lower and upper bounds.

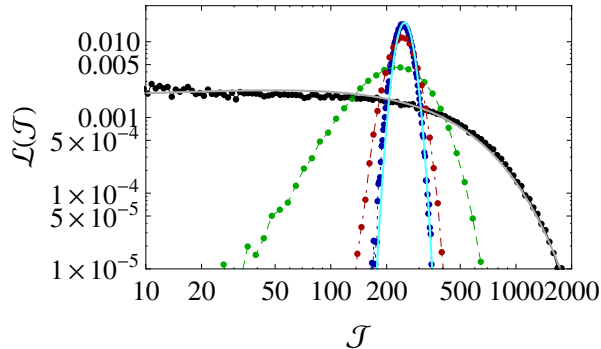


FIG. 8. Large Deviation Function,  $\mathcal{L}(\mathcal{J})$ , vs  $\mathcal{J}$  in log-log scale for shot-noise reservoir with Gaussian amplitude with canonical temperature  $T = 1$  for  $\Xi = 250$ ,  $m = 1, k = 1$ ,  $\gamma = 1$  and  $\sigma = \sqrt{2T/\lambda}$ . The points were obtained by numerical simulation following the legend:  $\lambda = 1/100$  (black),  $\lambda = 1/10$  (green),  $\lambda = 1$  (red) and  $\lambda = 10$  (blue). The grey line represents the low rate limit Eq. (67) and the cyan line represents the high rate limit Eq. (69).

## B. Power considerations

As discussed in Paper I — and in agreement with the entropy production of a non-equilibrium system — the dissipation, either accumulated or instantaneous,  $j_{\text{dis}} \equiv -\gamma v^2$ , plays the rôle of housekeeping heat and is always negative. On the other hand, the injected power  $j_{\text{inj}} \equiv \eta v$ , is two-sided. We address the reader to the EPAPS for the full expressions of the both cumulants. Herein, we first discuss the limiting cases of low and high shot-noise rates. In the former case, the moments are dominated by the terms proportional to  $\lambda$ ,

$$\lim_{\lambda \ll 1} \langle \langle j_{\text{inj}}^n \rangle \rangle = \lim_{\tau \rightarrow 0} \lambda \frac{\langle \Phi^{2n} \rangle}{2^n m^n} [\delta(\tau)]^{n-1}, \quad (70)$$

where the delta functions emerge for the white-noise nature of  $\eta$  as established by Eq. (4).

For the other limiting case of a high shot-noise rate,  $\lambda \rightarrow \infty$ , the moments are dominated the non-linearity of the system whereas in Ref. [16] explicit analytical calculations were made showing that the non-linear contribution to the cumulants of the fluxes are equal to zero.

by the term proportional to  $\lambda^n$  and the distribution of the injected power reads,

$$\lim_{\lambda \rightarrow \infty} p(j_{\text{inj}}) = p^*(j_{\text{inj}}) = \frac{1}{Z} \exp \left[ \frac{c}{f^2 \omega^2} j_{\text{inj}} \right] K_0 \left[ \frac{\sqrt{(c\chi)^2 + f^2 \omega^2}}{f^2 \omega^2 \chi} |j_{\text{inj}}| \right], \quad (71)$$

as we obtained for a Gaussian thermal reservoir case in Paper I. The parameters in Eq. (71) are defined as follows,

$$c = \lim_{\tau \rightarrow 0} [2m\delta(\tau)]^{-1}, \quad f = \sqrt{1 - mc^2\chi^2/T}, \quad (72)$$

$$\chi^2 = \lim_{\tau \rightarrow 0} 2\gamma T\delta(\tau), \quad \omega^2 = T/m,$$

and,

$$\mathcal{B} \equiv \frac{\sqrt{(c\chi)^2 + f^2 \omega^2}}{f^2 \omega^2 \chi}. \quad (73)$$

From Eq. (71), the fluctuation relation,

$$\ln \frac{p^*(j_{\text{inj}})}{p^*(-j_{\text{inj}})} \propto j_{\text{inj}}, \quad (74)$$

is easily obtained. For shot-noise processes, we can look whether this same relation is fulfilled. We carry that out recurring to the Edgeworth expansion, especially when  $\lambda$  is significant.

For instance, if the noise amplitude is symmetrical,  $f(\Phi) = f(-\Phi)$ , all the odd cumulants of  $\eta$  vanish. Adjusting the canonical temperature in Eq. (71) to the same value of a thermal temperature using Eq. (34), the first correction to the the distribution of the injected power relates only to the fourth-order cumulant,

$$\frac{p(j_{\text{inj}})}{p(-j_{\text{inj}})} = \exp \left[ \frac{2c}{f^2 \omega^2} j_{\text{inj}} \right] \frac{A_1^{(-)}(j_{\text{inj}}) K_0[\mathcal{B} j_{\text{inj}}] + A_2^{(-)}(j_{\text{inj}}) K_1[\mathcal{B} j_{\text{inj}}]}{A_1^{(+)}(j_{\text{inj}}) K_0[\mathcal{B} j_{\text{inj}}] + A_2^{(+)}(j_{\text{inj}}) K_1[\mathcal{B} j_{\text{inj}}]} + O(\Delta_6), \quad (75)$$

( $j_{\text{inj}} > 0$ ) with coefficients,

$$A_1^{(\pm)} = \{c^2 (c^2 + 6c\chi^2 + \chi^4) j_{\text{inj}}^2 + 2cf^2\omega^2 [3cj_{\text{inj}} + \chi^2(j_{\text{inj}} \pm 2c)] j_{\text{inj}} + f^4\omega^4 [3c\chi^2 + j_{\text{inj}}(j_{\text{inj}} \pm 4c)]\} j_{\text{inj}}^2 \Delta_4 + 3f^6\omega^6 [\Delta_4 + 8(f\omega j_{\text{inj}})^2], \quad (76)$$

$$A_2^{(\pm)} = 2\Delta_4 f^2 \omega^2 \chi \mathcal{B} \{3f^6\omega^6 + f^4\omega^4 (j_{\text{inj}} \pm 4c) j_{\text{inj}} + cf^2\omega^2 (3c \pm 2j_{\text{inj}} + \chi^2) j_{\text{inj}}^2 \pm 2c^2 (c + \chi^2) j_{\text{inj}}^3\} \quad (77)$$

and  $\Delta_n$  representing the difference between the  $n$ -th order cumulants of the injected power of the athermal and thermal reservoirs with  $K_n[x]$  representing the modified Bessel function of the second kind. Taking into account that the argument of the Bessel functions in Eq. (75) is always positive in the limit  $x \rightarrow \infty$ , we have  $K_n[x] = \sqrt{\pi/(2x)} \exp[-x]$  and we get,

$$\lim_{j_{\text{inj}} \rightarrow \infty} \ln \frac{p(j_{\text{inj}})}{p(-j_{\text{inj}})} = \frac{2c}{f^2 \omega^2} j_{\text{inj}} + \ln \frac{A_1^{(-)}(j_{\text{inj}}) + A_2^{(-)}(j_{\text{inj}})}{A_1^{(+)}(j_{\text{inj}}) + A_2^{(+)}(j_{\text{inj}})}, \quad (78)$$

or,

$$\ln \left[ \frac{\psi(j_{\text{inj}})}{\psi(-j_{\text{inj}})} \right] = \frac{2c}{f^2 \omega^2} j_{\text{inj}}. \quad (79)$$

In other words, we were able to recover the functional form of the thermal fluctuation relation if, instead of the probability density function, we consider the following function,

$$\psi(\pm |j_{\text{inj}}|) = \left[ A_1^{(\pm)}(|j_{\text{inj}}|) + A_2^{(\pm)}(|j_{\text{inj}}|) + O(\Delta_6) \right] p(\pm |j_{\text{inj}}|), \quad (80)$$

where the prefactor condenses the singular measure nature of the Poissonian shot-noise. It is worth calling attention that  $\psi(j_{\text{inj}})$  *does not* necessarily exhibit the properties of a probability density function.<sup>9</sup>

## V. FINAL REMARKS

In this paper, using techniques of time averaging over the noise and the final-value theorem, we have extended to athermal reservoirs the analysis of the impact of nonlinearities on the long-term thermostistical properties of massive one-particle systems with mass  $m$ . The athermal nature of the reservoir is analytically represented by a (Poissonian) shot-noise with rate,  $\lambda$ , and random amplitude,  $\Phi$ . There exist problems of that ilk galore, *e.g.*, several solid state systems, resistor-inductor-capacitor circuits, surface diffusion and low vibrational motion with adsorbates, biological motors in which shot noise mimics the non-equilibrium stochastic hydrolysis of adenosine triphosphate, granular gases and molecular dynamics employing the Andersen thermostat among many others [6]-[14]. After recasting previous results of ours on the statistics of the position and the velocity for the linear case [17], we have moved on to energetic considerations over

---

<sup>9</sup> Actually, from the Edgeworth expansion we learnt that  $\psi(j_{\text{inj}})$  is not a probability density function.

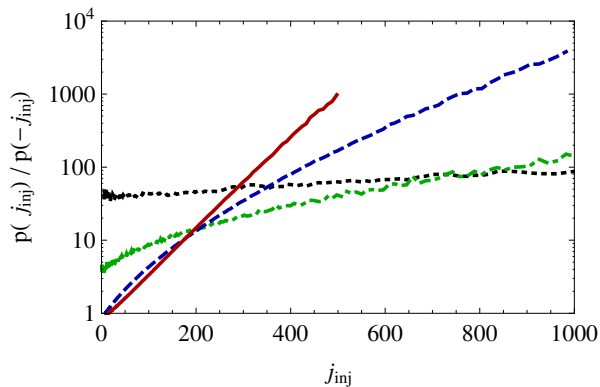


FIG. 9. Fluctuation relation of the injected power for a Poissonian athermal reservoir with an exponentially distributed amplitude in log-linear scale. Each curve was obtained from data sets of  $10^{10}$  elements numerically obtained. The mechanical parameters are  $m = 1$ ,  $k_1 = 1$ ,  $\gamma = 1$  and temperature  $T = 1/10$ . The legend is the following: black dotted line ( $\lambda = 1/100$ ), green dot-dashed line ( $\lambda = 1/10$ ), blue dashed line ( $\lambda = 1$ ) and red full line ( $\lambda = 10$ ). The cases  $\lambda = 1/10$ ,  $\lambda = 1$  evince the asymptotic exponential behaviour given by Eq. (78) whereas the case  $\lambda = 10$  is already very close to the thermal case with a nearly perfect exponential dependence.

non-linear systems. Despite of the fact that the second moment of the velocity — and thus the average kinetic energy — is insensitive to the non-linearity of the potential, its further moments depend on  $k_3$ . That is at odds with the results for the thermal reservoir for which the form of the potential only plays a rôle during the transient.

From the average kinetic energy, we established an effective temperature,  $T$ , to that (actually) athermal system and whence we have set up an analogous fluctuation-dissipation relation [Eq. (21)] connecting  $T$  and the shot-noise amplitude,  $\Phi$ , with the dissipation,  $\gamma$ , produced by the medium in which the motion happens. Along these lines, the white shot-noise is reckoned as an athermal internal reservoir for which the dissipation and fluctuations could have the same microscopic origin, a scenario that fits for granular gases and molecular dynamics under Andersen thermostats. Next, to evaluate the steady state potential energy,  $\mathcal{V}$ , we have developed a recipe to obtain in a fast diagrammatic way, the non-linear first order contribution to any moment of the position. This means that besides the purely non-linear value of  $k_3 \langle x^4 \rangle / 4$ , the non-Gaussian nature of the athermal reservoir also affects the harmonic contribution  $k_1 \langle x^2 \rangle / 2$  of the potential. In the limit of

a high shot-noise rate [a ratio  $\gamma/(m\lambda)$  as large as 100 is already enough], the form of the stationary distribution,  $p(x)$ , depends on the symmetry of the noise. On the one hand, when the shot-noise is single sided — mimicking the case of a work reservoir as occurs in several molecular motors [30] — we have  $\langle x \rangle \neq 0$  (for a fixed temperature,  $\langle x \rangle_1 \propto \sqrt{\lambda}$ ) and the distribution does not converge to  $p(x) \propto \exp[-(k_1 x^2/2 + k_3 x^4/4)/T]$ . Although the introduction of the non-linearity decreases the value of  $\langle x \rangle$ , it also reduces the value of  $\langle\langle x^2 \rangle\rangle$  making the distribution narrower. On the other hand, when the noise is symmetric, the particle always moves around  $x = 0$  and in increasing  $\lambda$  we approach the expected Boltzmann weight.

Afterwards, we have learnt that the non-Gaussian terms in  $\mathcal{V}$  are proportional to the cumulants of the position and consequently to the cumulant of the noise. In Ref. [15], we conveyed that for athermal reservoirs the higher (than second) order cumulants are understood as sources of energy of higher-order, a reasoning that was also corroborated by Kazanawa and coworkers [13]. Thence, taking into consideration past and present results, we have introduced the concept of  $n$ -th order temperature,  $\mathcal{T}_n$ , [Eq. (40)] that retrieves the canonical temperature when  $n = 2$ . For  $n \neq 2$ , *the temperatures  $\mathcal{T}_n$  are intimately related to the mechanical features of the system and are only different from zero when the reservoir is non-Gaussian*, which leads to the emergence of non-zero higher-order cumulants. Using that definition, the potential energy is written in the form of a combination of temperatures that resembles an extended form of the equipartition theorem. This form of writing down the energetic results has allowed us to enlarge the set of response functions, especially the response of the energy to changes in the  $n$ -th order temperature [Eq. (46)] so that for  $n = 2$  it yields the (standard) specific heat. The calculation of the higher-order specific heats evinces that the energy of the system is only sensitive to changes in the ( $n \neq 2$ )-th order cumulants of the reservoir (and hence  $\mathcal{T}_{n \neq 2}$ ) when we are in the presence of non-linearities. Along the time independent analysis, we have surveyed the properties of the total injected and dissipated fluxes,  $\mathcal{J}_{\text{inj}(\text{dis})}$ , which have the same statistics. For an athermal reservoir, the former can be either a heat or a work flux whereas the former is always a heat flux. The distribution of these time-dependent quantities suits the concept of a large deviation. The long-term distribution of the fluxes, a large deviation function, matches the thermal case when the rate of the

injection,  $\lambda$ , tends to infinity and the noise approaches a continuous measure,  $\mathcal{L}^{(u)}(\mathcal{J})$ . In the opposing limit,  $\lambda \ll 1$ , we have found the respective large deviation function,  $\mathcal{L}^{(l)}(\mathcal{J})$ , which differs from the continuous noise measure limit. These two situations, act as lower and upper bounds of the large deviation function of the fluxes in an athermal system. For other general cases, we have been unable to find closed expressions because of the intricateness of the cumulants. Nonetheless, these limiting distributions can be used to build an approximation of  $\mathcal{L}(\mathcal{J})$  for any value of  $\lambda$ .

Last, we have analysed the impact of the athermal nature of the reservoir in the fluctuation-relation for the power injected by the reservoir,  $j_{\text{inj}}$ . As shown by Eq. (78), we have verified that the behaviour of  $\ln [p(|j_{\text{inj}}|)/p(-|j_{\text{inj}}|)]$  is still proportional to  $|j_{\text{inj}}|$  in the limit  $|j_{\text{inj}}| \rightarrow \infty$  because the contribution from the singular measure of the reservoir is sub-exponential giving only a significant contribution for small values of  $|j_{\text{inj}}|$ . Notwithstanding, if one considers the introduction of a probability *functional*,  $\psi$ , *i.e.*, a function that is function of the probability density function  $p(j_{\text{inj}})$ , one recovers the standard form of the (thermal) fluctuation relation. The deviation of  $\psi$  from the identity functional  $\mathbb{I} : p(j_{\text{inj}}) \rightarrow p(j_{\text{inj}})$  can thus be interpreted as a thermostistical measure of the athermalness of the reservoir.

To conclude the analysis, we match the powers  $\langle j_{\text{inj}} \rangle$  and  $\langle j_{\text{dis}} \rangle$  with the entropy production relation  $dS/dt = \Pi - \Psi$ , namely with the entropy production,  $\Pi$ , and entropy exchange  $\Psi$ , respectively. Using the canonical temperature and assuming  $\mathcal{J} \equiv \Sigma T$ , where  $\Sigma$  denotes entropy, we are able to identify the long-term behaviour  $\Pi = \Psi = \gamma/m$  which is found for the thermal case white-noises as well. It must be stressed that similarities end when the system has non-linearities, as we shown in this paper.

Regarding future work, two prevalent ideas come out; the first one is related to the extension of the present analysis to dimers and polymers. Second, as we can understand, seeing that non-linearity does not influence  $\langle v^2 \rangle$ , for a non-linear system in contact with an athermal non-Gaussian reservoir, standard measure of the fluxes do not take into consideration the sources of energy of higher-order — represented by the cumulants of higher-order — that eventually pass unnoticed. Therefore, it is certainly interesting to shed some light on effective ways of describing them and possibly related fluctuation relations.

## ACKNOWLEDGMENTS

We would like to thank the partial funding from FINEP [contract No. PUC-Infra 1580/10], FAPERJ [contract No. APQ1-110.635/2014] and CNPq [contract No.s 481640/2011-8 and 308737/2013-0].

## Appendix A: Diagrammatic for first order non-linear contributions

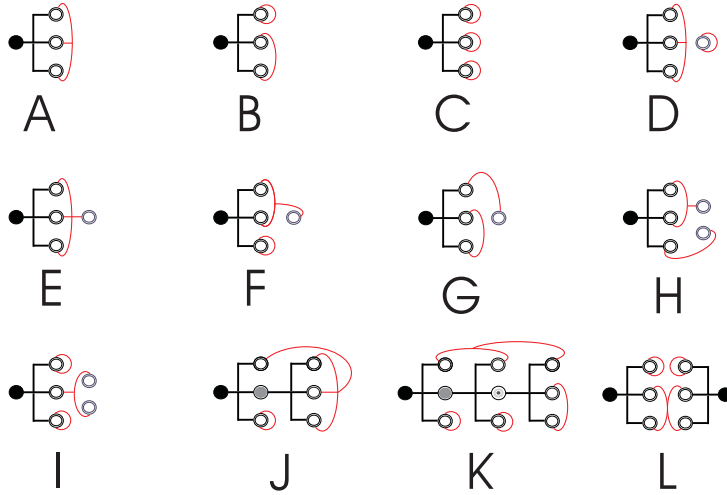


FIG. 10. Diagrams used in the explanation of the recipe presented in Appendix A.

The present appendix aims to introduce the fast-track 5-step method we established to find the first order contributions of any statistical moment of the position. To explain it, we avail ourselves of Figure 10:

1. Count the number of lower order  $\tilde{x}$ s [Eq. (8) and Fig. 1] that are involved in the calculation — *i.e.*, the full black dots and the hollow dots that are not part of a pitchfork — and verify how they link between them. This establishes factors  $C_j^l$  defined in Eq. (??) that composed the term. For instance:

- diagrams A, B and C, which yield  $\bar{x}_{\text{nl}}$ , only involve one lower order  $\tilde{x}$  and therefore we will only have terms proportional to  $C_0^0$ ;

- diagrams D and E , which contribute to  $\overline{x^2_{nl}}$ , have two lower order  $\tilde{x}$ s, but yield different results. in spite of D have them detached and thus it is proportional to  $[C_0^0]^2$  whereas the diagram E that has both connected gives rise to  $C_j^1$ .
2. Check how the higher order  $\tilde{x}$ s — *i.e.*, hollow dots that belong to the pitchfork — link between them and compute its combinatorics irrespective of existing links to other (higher order) dots. In other words:
    - if the three pitchfork dots are linked, we have a factor  $3! = 6$ , like it occurs for diagrams A, D and E;
    - if two pitchfork dots are connected the factor equal  $2!$  as for B, F, G and H (that contributes to  $\overline{x^3_{nl}}$ );
    - if all the pitchfork are detached the combinatorial factor is 1, as we have for diagrams C and I (that contributes to  $\overline{x^3_{nl}}$ ).
  3. Define the another factor taking into consideration how the higher-order terms are connected:
    - the three pitchfork dots links yield  $([3, 0] [2, 1] [1, 2] [0, 3])^{-1}$ ;
    - two pitchfork dots connected give  $([2, 0] [1, 1] [0, 2])^{-1} ([1, 0] [0, 1])^{-1}$ ;
    - all the pitchfork not linked result in  $([1, 0] [0, 1])^{-1} ([1, 0] [0, 1])^{-1} ([1, 0] [0, 1])^{-1}$ .
  4. Adjust the factors determined in the previous point taking into consideration the factors  $C_j^1$  of point 1. Let us have a look at some illustrative examples:
    - in diagram D, the pitchfork dots are all connected between them and there is no further connection to other dots, thus the factor of point 3. remains unchanged. To obtain its end value we just need to multiply it by  $[C_0^0]^2$ ;
    - in diagram E, the entire pitchfork is connected to a higher order term and from point 1. we have learnt that there exists a factor  $C_j^1$ . This implies that the factor is changed accordingly to  $([4, 0] [3, 1] [2, 2] [1, 3])^{-1}$  for the term with coefficient  $C_0^1$  and  $([3, 1] [2, 2] [1, 3] [0, 4])^{-1}$  for the term with coefficient  $C_1^1$ ;

- in diagram I, the pitchfork dots are independent between them but one of them is connected to other two lower order dots. The general panorama gives  $C_j^2$ . In accordance with that we have said, the diagram contribution is proportional to  $([3, 0] [2, 1])^{-1} ([1, 0] [0, 1])^{-1} ([1, 0] [0, 1])^{-1}$ ,  $([2, 1] [1, 2])^{-1} ([1, 0] [0, 1])^{-1} ([1, 0] [0, 1])^{-1}$ ,  $([2, 1] [1, 2])^{-1} ([1, 0] [0, 1])^{-1} ([1, 0] [0, 1])^{-1}$  and  $([1, 2] [0, 3])^{-1} ([1, 0] [0, 1])^{-1} ([1, 0] [0, 1])^{-1}$ .
- in diagram G, we have two lower order dots connected to the pitchfork; however, one is connected to an isolated dot and the other one to the remaining pair of higher order dots. For this reason, corrections to the factor  $([2, 0] [1, 1] [0, 2])^{-1} ([1, 0] [0, 1])^{-1}$  from this links are distinguishable by the values of  $\zeta_{\pm}$ . Therefore, instead of simply using the notation  $C_j^2$ , we will use  $C_{\{j\}}^2$ , where  $\{j\}$  precisely signals the different partitions. For this diagram is have,

$$\begin{aligned} \text{G} \propto & \frac{C_{\{0,0\}}^2}{([3, 0] [2, 1] [1, 2]) ([2, 0] [1, 1])} + \frac{C_{\{1,0\}}^2}{([2, 1] [1, 2] [0, 3]) ([2, 0] [1, 1])} \quad (\text{A1}) \\ & \frac{C_{\{0,1\}}^2}{([3, 0] [2, 1] [1, 2]) ([1, 1] [0, 2])} + \frac{C_{\{1,0\}}^2}{([2, 1] [1, 2] [0, 3]) ([1, 1] [0, 2])}. \end{aligned}$$

- It is important to stress that  $C_{\{j\}}^l$  is still given by Eq. (??) with  $j = \sum_i j_i$ .

5. Obtain the proportionality constant for each coefficient,  $i$ . For the  $n$ -th order moment non-linear contribution we have,

$$g_i \frac{\lambda^{c_i} \prod_{o=1}^{c_i} \langle \Phi^{\nu_o} \rangle}{m^{n+2}}, \quad (\text{A2})$$

where,

- $c_i$  represents the number grouplets in the diagram  $i$  (which runs from 1 to  $n + 2$ );
- $\nu_o$  is the moment of the amplitude, *i.e.*, the number  $\nu$  of dots connected in the  $o$  grouplet formed in diagram  $i$  that contains  $c_i$  grouplets;
- $g_i$  is the degeneracy defined the corresponding Faà di Bruno formula relating the statistical moments with cumulants multiplied by  $(-1)$  if there is a grouplet composed of and only two) two higher order dots from the pitchfork.

Let us briefly mention the computation of higher-orders in  $k_3$  can be carried out along this same spirit. In that case, two different cases emerge. If the higher order results from a single cascade of pitchforks — *e.g.*, J and K — some modifications to the “diagrammar” we established can be introduced without much difficulty. Things get quite more intricate when the terms emerge from different cascades as befalls in diagram L. In spite of being possible to write a recipe to those cases as well, the combinatorial intricateness of its outcome has little physical interpretation and falls off the scope of the present work.

### Appendix B: Expressions for cumulants

We list below some exact results for the cumulants of position and velocity:

$$\overline{\overline{x^n}} = n! \frac{(-1)^{n+1}}{\prod_{j=0}^n [(n-j), j]} \frac{\lambda \langle \Phi^n \rangle}{m^n}. \quad (\text{B1})$$

where,

$$[a, b] \equiv a \zeta_+ + b \zeta_-. \quad (\text{B2})$$

Yet performing the computations for Sec. 2, we have realised that, it is best to recast Eq. (B1) in the form,

$$\begin{aligned} \overline{\overline{x^n}} &= \sum_{j=0}^{n-1} \binom{n-1}{j} \frac{(-1)^j}{\prod_{l=0}^1 [(n-j-l), (j+l)]} \frac{\lambda \langle \Phi^n \rangle}{m^n [1, -1]^{n-1}} \\ &= \frac{\lambda \langle \Phi^n \rangle}{m^n} \sum_{j=0}^{n-1} \binom{n-1}{j} C_j^{n-1}, \end{aligned} \quad (\text{B3})$$

with,

$$C_j^n \equiv \frac{(-1)^j}{[1, -1]^n \prod_{l=0}^1 [(n-j-l+1), (j+l)]}. \quad (\text{B4})$$

Equation (B3) enlightens the contributions for the cumulants of the position. For instance, for the second order cumulant, we have got two terms, each coming from one of the zeroes,  $\zeta_{\pm}$ ; the third order cumulant has got its three terms related to the combinations of the zeroes  $\zeta$ , *i.e.*,  $(\zeta_+, \zeta_+)$ ,  $(\zeta_+, \zeta_-)$ ,  $(\zeta_-, \zeta_-)$ ; and so forth.

Regarding the cumulants of the velocity, in the harmonic case we got,

$$\begin{aligned} \overline{v^n} &= \lim_{z, \epsilon \rightarrow 0} \int_{-\infty}^{\infty} \prod_{j=1}^n \frac{dq_j}{2\pi} (i q_j + \epsilon) \frac{z}{z - \sum_{l=1}^n (i q_l + \epsilon)} \left\langle \left\langle \prod_{l=1}^n \frac{\tilde{\eta}(i q_l + \epsilon)}{R(i q_l + \epsilon)} \right\rangle \right\rangle, \quad (\text{B5}) \\ &= \sum_{j=0}^{n-1} (-1)^{j-1} \binom{n-1}{n-j-1} \frac{\zeta_+^{n-j-1} \zeta_-^j [(n-j-1), j]}{\prod_{l=0}^1 [(n-j-l), (j+l)]} \frac{\lambda \langle \Phi^n \rangle}{m^n [1, -1]^{n-1}}. \end{aligned}$$

Using the series expansions of hypergeometric functions [23], we have found that Eq. (B5) can be rewritten as,

$$\begin{aligned} \overline{v^n} &= \frac{\lambda \langle \Phi^n \rangle}{\zeta_- [\zeta_+ - \zeta_-]} \left( \frac{\zeta_+}{m} \right)^n \left[ \frac{\zeta_-}{\zeta_+} \right]^{\frac{\zeta_+ n}{\zeta_+ - \zeta_-}} \times \\ &\quad \left\{ B_{\frac{\zeta_-}{\zeta_+}} \left[ -\frac{\zeta_+ n}{\zeta_+ - \zeta_-}, n \right] - B_{\frac{\zeta_-}{\zeta_+}} \left[ 1 - \frac{\zeta_+ n}{\zeta_+ - \zeta_-}, n \right] \right\}. \quad (\text{B6}) \end{aligned}$$

where  $B_a [b, c]$  represents the incomplete Beta function.

### Appendix C: General Proof of $\overline{v^2_{nl}} = 0$

An important property can be verified for the non-linear contribution for the velocity variance, namely

$$\overline{v^2_{nl}} = 0$$

On first order on  $k_3$ ,

$$\begin{aligned} \overline{v^2_{nl}} &= \lim_{z \rightarrow 0} \lim_{\epsilon \rightarrow 0} \int \prod_{j=1}^2 \frac{dq_j}{2\pi} \frac{z}{z - (i q_1 + i q_2 + 2\epsilon)} \langle \tilde{x}(i q_1 + \epsilon) \tilde{x}(i q_2 + \epsilon) \rangle \\ &= \lim_{z \rightarrow 0} \lim_{\epsilon \rightarrow 0} \lim_{\alpha \rightarrow 0} -2 k_3 \int \prod_{j=1}^5 \frac{dq_j}{2\pi} \frac{z}{z - (i q_1 + i q_2 + 2\epsilon)} \frac{(i q_1 + \epsilon) (i q_2 + \epsilon)}{R(i q_1 + \epsilon) R(i q_2 + \epsilon) \prod_{i=3}^5 R(i q_i + \alpha)} \\ &\quad \times \frac{1}{i q_1 + \epsilon - \sum_{j=3}^5 (i q_j + \alpha)} \left\langle \prod_{j=2}^5 \tilde{\eta}(i q_j + \alpha) \right\rangle. \quad (\text{C1}) \end{aligned}$$

- 
- [1] H. Mori, Prog. Theor. Phys. **33**, 423 (1965); S. R. de Groot and P. Mazur *Non-equilibrium Thermodynamics* (North-Holland, Amsterdam, 1984); R. Zwanzig, *Nonequilibrium Statis-*

- tical Mechanics* (Oxford University Press, Oxford, 2001); an nice synopsis on this subject can be found in: P. Hänggi and F. Marchesoni, *Chaos* **15**, 026101 (2005).
- [2] H. Mori, *Prog. Theo. Phys.* **33**, 423 (1965).
  - [3] C. W. Gardiner, *Handbook of Stochastic Methods for Physics, Chemistry and the Natural Sciences* (Springer-Verlag, Berlin, 1983).
  - [4] N. G. van Kampen, *Stochastic Processes in Physics and Chemistry* (North-Holland, Amsterdam, 2007).
  - [5] D. Applebaum, *Lévy Processes and Stochastic Calculus* (Cambridge University Press, Cambridge, 2004).
  - [6] T. S. Druzhinina, S. Hoepfner and U. S. Schubert, *Nano Lett.* **10**, 4009 (2010); A. A. Balandin, *Nat. Mater.* **10**, 569 (2011).
  - [7] Sh. Kogan, *Electronic Noise and Fluctuations in Solids* (Cambridge University Press, Cambridge, 1996); Ya. M. Blanter and M. Büttiker, *Phys. Rep.* **336**, 1 (2000); Y. Demirel, *Nonequilibrium Thermodynamics: Transport and Rate Processes in Physical and Biological Systems* (Elsevier, Amsterdam, 2002).
  - [8] R. Martínez-Casado, J. L. Vega, A. S. Sanz and S. Miret-Artés, *Phys. Rev. Lett.* **98**, 216102 (2007); R. Martínez-Casado, J. L. Vega, A. S. Sanz and S. Miret-Artés, *Phys. Rev. E* **75**, 051128 (2007).
  - [9] T. Czernik, J. Kula, J. Luczka and P. Hänggi, *Phys. Rev. E* **55**, 4057 (1997); J. C. M. Gebhardt, A. E.-M. Clemen, J. Jaud and M. Rief, *Proc. Natl. Acad. Sci. USA* **103**, 8680 (2006).
  - [10] A. Baule and E. G. D. Cohen, *ibid.* **79**, 030103 (2009).
  - [11] H. C. Andersen, *J. Chem. Phys.* **72**, 2384 (1980); Ph. H. Hünenberger, *Adv. Polym. Sci.* **173**, 105 (2005).
  - [12] P. Eshuis, K. van der Weele, D. Lohse and D. van der Meer, *Phys. Rev. Lett.* **104**, 248001 (2010).
  - [13] K. Kanazawa, T. Sagawa and H. Hayakawa, *Phys. Rev. E* **87**, 052124 (2013).
  - [14] K. Kanazawa, T. G. Sano, T. Sagawa and H. Hayakawa, *Phys. Rev. Lett.* **114**, 090601 (2015).
  - [15] W. A. M. Morgado and S. M. Duarte Queirós, *Phys. Rev. E* **86**, 041108 (2012).

- [16] W. A. M. Morgado and S. M. Duarte Queirós, *Phys. Rev. E* **90**, 022110 (2014).
- [17] W. A. M. Morgado and S. M. Duarte Queirós and D. O. Soares-Pinto, *J. Stat. Mech.* (2011) P06010.
- [18] P. Hänggi, K. E. Shuler and I. Oppenheim, *Physica A* **107**, 143 (1981).
- [19] J. Łuczka, T. Czernik and P. Hänggi, *Phys. Rev. E* **56**, 3968 (1997).
- [20] D. O. Soares-Pinto and W. A. M. Morgado, *Physica A* **365**, 289 (2006).
- [21] B. van der Pol and H. Bermmer, *Operational Calculus Based on the Two-Sided Laplace Integral* (Cambridge University Press, Cambridge, 1950). For a pedagogical approach: E. Gluskin, *Eur. J. Phys.* **24**, 591 (2003).
- [22] See Supplemental Material at TO BE INSERTED BY THE EDITORIAL OFFICE for detailed calculations concerning equations the potential energy.
- [23] I. S. Gradshteyn and I. M. Ryzhik, *Table of Integrals, Series and Products* (Academic Press, New York, 2007); <http://functions.wolfram.com>
- [24] W. A. M. Morgado and E. R. Mucciolo, *Physica A* **311**, 150 (2002); S. M. Duarte Queirós, *Braz. J. Phys.* **38**, 203 (2008).
- [25] R. Klages, W. Just and C. Jarzynski (editors) *Nonequilibrium Statistical Physics of Small Systems: Fluctuation Relations and Beyond* (Wiley-VCH Verlag, Weinheim, 2013).
- [26] <http://mathworld.wolfram.com/RawMoment.html>
- [27] J.S. Lee, C. Kwon and H. Park, *Phys. Rev. E* **87**, 020104(R) (2013).
- [28] J. Gärtner, *Th. Prob. Appl.* **22**, 24 (1977); R. S. Ellis, *Ann. Prob.* **12**, 1 (1984); H. Touchette, *Phys. Rep.* **478**, 1 (2009).
- [29] J. Farago, *J. Stat. Phys.* **107**, 781 (2002).
- [30] A. B. Kolomeisky and M. E. Fisher, *Annu. Rev. Phys. Chem.* **58**, 675 (2007).

NOTAS DE FÍSICA é uma pré-publicação de trabalho original em Física.  
Pedidos de cópias desta publicação devem ser enviados aos autores ou ao:

Centro Brasileiro de Pesquisas Físicas  
Área de Publicações  
Rua Dr. Xavier Sigaud, 150 – 4<sup>o</sup> andar  
22290-180 – Rio de Janeiro, RJ  
Brasil  
E-mail: [socorro@cbpf.br](mailto:socorro@cbpf.br)/[valeria@cbpf.br](mailto:valeria@cbpf.br)  
<http://portal.cbpf.br/publicacoes-do-cbpf>

NOTAS DE FÍSICA is a preprint of original unpublished works in Physics.  
Requests for copies of these reports should be addressed to:

Centro Brasileiro de Pesquisas Físicas  
Área de Publicações  
Rua Dr. Xavier Sigaud, 150 – 4<sup>o</sup> andar  
22290-180 – Rio de Janeiro, RJ  
Brazil  
E-mail: [socorro@cbpf.br](mailto:socorro@cbpf.br)/[valeria@cbpf.br](mailto:valeria@cbpf.br)  
<http://portal.cbpf.br/publicacoes-do-cbpf>